Transfer-printing enables multi-material assembly of integrated photonic systems

Dimitars Jevtics[1], Jack A. Smith[1], John McPhilimy[1], Benoit Guilhabert[1], Paul Hill[1], Charlambos Klitis[2], Marc Sorel[2], Antonio Hurtado[1], Martin D. Dawson[1], Michael J. Strain[1]

1.Institute of Photonics, Dept. of Physics, University of Strathclyde, Glasgow G1 1RD, UK
2.School of Engineering, University of Glasgow, Glasgow G12 8QQ, UK
Author e-mail address: dimitars.jevtics@strath.ac.uk

Abstract: Hybrid integration of photonic membrane and nanowire devices from multiple material platforms is demonstrated using high-accuracy transfer printing. The deterministic assembly technique enables serially printed devices with separations as low as 100 nm.

OCIS codes: 130.0130, 220.0220, 350.4238

In the past decade, the fabrication of photonic systems beyond the limits imposed by wafer growth considerations has become widely investigated as a basis for heterogeneous device integration on a single chip [1]. The ability to mix-and-match photonic devices and assemble those into systems makes the transfer-printing (TP) approach an appealing technique for heterogeneous integration. Although, a great deal of proof-of-concept results showing the capabilities of TP have been reported to date, demonstrations have typically focused on the integration of devices from a single material platform onto a host chip [2–6]. Full exploitation of this method allows for the integration of multiple material devices within an area comparable with the device footprint, which will be important for applications such as hybrid quantum photonic integrated circuits [7]. A significant challenge for TP integration at these scales is the serial printing of multiple devices within a small footprint, where each print step does not disturb already situated devices.

In this work, we discuss our recent results in heterogeneous integration by TP using automated nanoscale accuracy alignment system [8] and present multi-material integrated photonic components with a footprint in the order of the device size. The schematic diagram in Fig. 1 depicts the assembly of a photonic system using the TP process: (1) a target device/component is captured from its growth substrate using an elastomeric μ-stamp. To support high-yield integration, custom printing heads on the μ-stamp are shaped to match the top surface of target devices. Furthermore, this also ensures that the transferred devices will not interact with the already assembled system. (2) the captured device is aligned with a receiving area on a host substrate. (3) the target device is then released at a target location. (4) the process can also be repeated by utilizing various components and materials in a mix-and-match fashion to assemble a photonic system.

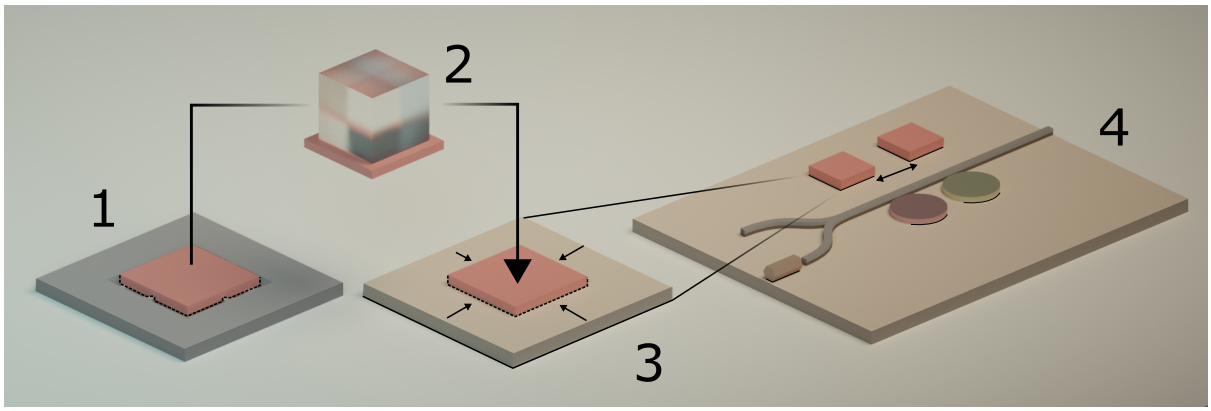

Fig. 1: Schematic diagram showing steps of TP process: (1) a device with sacrificial anchors is fabricated. (2) a polymeric μ-stamp captures the selected device from its growth substrate. (3) the device is released onto a host (non-native) surface on the target location. (4) The combination of various materials and photonic elements can be assembled into an on-chip system using the TP process.

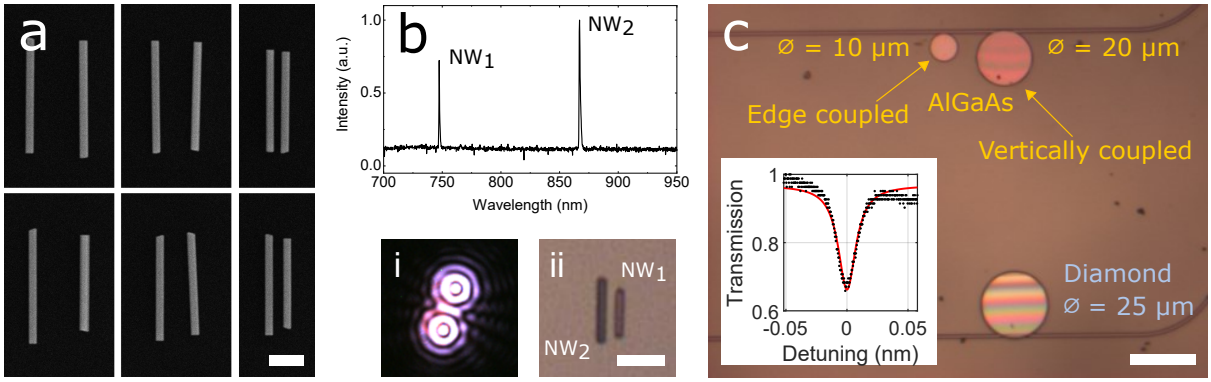

Fig. 2: (a) A set of InP TP NW pairs with target separations ranging from 1 – 3 μm. Scale bar: 1 μm. (b) Spectrum showing dual-color lasing of a laterally positioned NW laser pair. Insets show (i) dark-field and (ii) brightfield micrographs of GaAs/AlGaAs and InP NW lasers on SiO_2 substrate. Scale bar: 5 μm. (c) Transfer-printed AlGaAs and Diamond μ-disk resonators coupled with GaN waveguides on Sapphire substrate. Inset shows resonance fit for the Diamond μ-disk device. Scale bar: 25 μm.

The enhanced capabilities of the TP system enable assembling multi-material photonic systems with reduced separations between individual elements or/and devices. Semiconductor nanowire (NW) laser pairs (diameter $\sim$ 260 nm, lengths $\sim$ 10 μm), shown in Fig. 2(a), were individually positioned and laterally aligned with target separations of 3, 2, and 1 µm for the three respective columns. The average estimated accuracy for the closely aligned pairs is 115 nm with standard deviation of 619 nm (3σ). These results are also comparable with those used for benchmarking of the automated alignment technique [8]. From a practical point of view, this work can be extended to demonstrating dual-color lasing emission using laterally aligned NW pairs, see results in Fig. 2(b). The same integration method was used to integrate InP and GaAs/AlGaAs NW devices onto SiO_2 substrate. The target edge-to-edge separation was set to 1.5 μm to avoid mode interaction between the two elements. Upon the optical excitation, both devices showed single-mode lasing emission at room temperature. Furthermore, Fig. 2(c) shows two TP AlGaAs and Diamond μ-disk resonators on a GaN-on-sapphire chip. The transferred resonators were coupled onto GaN waveguides with evanescent field coupling achieved through lateral or vertical positioning of the disk, highlighting the freedom afforded by the TP assembly method. The inset in Fig. 2(c) shows a resonance fit for the diamond µ-disk device, which was characterized from 1540 – 1600 nm. A Q-factor of 91 000 was measured for the vertically coupled μ-disk, illustrating that the TP process does not increase intrinsic losses of the transferred device [9].

In conclusion, the presented work shows great promise for using the TP technique with an automated alignment algorithm for realizing dense hybrid on-chip photonic systems and combining various materials and devices onto a single chip. The significant advantage of the technique is the integration mechanism that does not damage the printed devices, does not require post-processing, and offers nanoscale positioning accuracies [3, 8, 9]. Furthermore, by custom shaping of the polymeric µ-stamps serial printing of devices from multiple donor chips can be achieved without disturbing preassembled components on the chip.

References

1. B. Corbett, R. Loi, W. Zhou, D. Liu, and Z. Ma, Prog. Quantum Electron. **52**, 1–17 (2017).
2. A. J. Trindade, B. Guilhabert, D. Massoubre, D. Zhu, N. Laurand, E. Gu, I. M. Watson, C. J. Humphreys, and M. D. Dawson, Appl. Phys. Lett. **103**, 253302 (2013).
3. K. Peng, D. Jevtics, F. Zhang, S. Sterzl, D. A. Damry, M. U. Rothmann, B. Guilhabert, M. J. Strain, H. H. Tan, L. M. Herz, L. Fu, M. D. Dawson, A. Hurtado, C. Jagadish, and M. B. Johnston, Science **368**, 510–513 (2020).
4. B. Guilhabert, A. Hurtado, D. Jevtics, Q. Gao, H. H. Tan, C. Jagadish, and M. D. Dawson, ACS Nano **10**, 3951–3958 (2016).
5. D. Jevtics, A. Hurtado, B. Guilhabert, J. McPhillimy, G. Cantarella, Q. Gao, H. H. Tan, C. Jagadish, M. J. Strain, and M. D. Dawson, Nano Lett. **17**, 5990–5994 (2017).
6. J. McPhillimy, B. Guilhabert, C. Klitis, M. D. Dawson, M. Sorel, and M. J. Strain, Opt. Express **26**, 16679 (2018).
7. J. Wang, F. Sciarrino, A. Laing, and M. G. Thompson, Nat. Photonics **14**, 273–284 (2019).
8. J. McPhillimy, D. Jevtics, B. J. E. Guilhabert, C. Klitis, A. Hurtado, M. Sorel, M. D. Dawson, and M. J. Strain, ACS Appl. Nano Mater. **3**, 10326–10332 (2020).
9. B. Guilhabert, J. McPhillimy, S. May, C. Klitis, M. D. Dawson, M. Sorel, and M. J. Strain, Opt. Lett. **43**, 4883 (2018).